Technical note: Fu-Liou-Gu and Corti-Peter model performance evaluation for radiative retrievals from cirrus clouds

S. Lolli[1,2], J. R. Campbell[3], J. Lewis[1], Y. Gu[4], E. J. Welton[5]

[1]NASA GSFC-JCET, Code 612, 20771 Greenbelt, MD, USA

[2] CNR-IMAA, Istituto di Metodologie per l'Analisi Ambientale, Potenza, Italy

[3] Naval Research Laboratory, Monterey, CA, USA

[4] UCLA, Los Angeles, CA, USA

[5] NASA GSFC, Code 612, 20771 Greenbelt, MD, USA

Corresponding author: slolli@umbc.edu

Abstract

We compare, for the first time, the performance of a simplified atmospheric radiative transfer algorithm package, the Corti-Peter (CP) model, versus the more complex Fu-Liou-Gu (FLG) model, for resolving top-of-the-atmosphere radiative forcing characteristics from single layer cirrus clouds obtained from the NASA Micro Pulse Lidar Network database in 2010 and 2011 at Singapore and in Greenbelt, Maryland, USA in 2012. Specifically, CP simplifies calculation of both clear-sky longwave and shortwave radiation through regression analysis applied to radiative calculations, which contributes significantly to differences between the two. The results of the intercomparison show that differences in annual net TOA cloud radiative forcing can reach 65%. This is particularly true when land surface temperatures are warmer than 288 K, where the CP regression analysis becomes less accurate. CP proves useful for first-order estimates of TOA cirrus cloud forcing,

but may not be suitable for quantitative accuracy, including the absolute sign of cirrus cloud daytime TOA forcing that can readily oscillate around zero globally.

1. Introduction

Cirrus clouds play a fundamental role in atmospheric radiation balance and their net radiative effect remains unclear (IPCC 2013; Berry and Mace 2014; Campbell et al. 2016; Lolli et al. 2017). Feedbacks between cirrus dynamic, microphysical and radiative processes are poorly understood, with ramifications across a host of modeling interests and temporal/spatial scales (Liou 1985; Khvorostyanov and Sassen 1998). Simply put, different models parameterize ice formation in varied, yet relatively simplified, ways that impact how cirrus are resolved, and how their macro/microphysical and radiative properties are coupled with other atmospheric processes (e.g., Comstock et al. 2001; Immler et al. 2008). Consequently, models are very sensitive to small changes in cirrus parameterization (Soden and Donner 1994; Min et al. 2010; Dionisi et al., 2013).

Cirrus clouds are the only tropospheric cloud genus that either exerts a positive or negative top-of-the-atmosphere (TOA) cloud radiative forcing effect (CRE) during daytime. All other clouds exert a negative daytime TOA CRE. Cirrus clouds exerting negative net TOA CRE cool the earth-atmosphere system and surface below them. This occurs as the solar albedo term is greater than the infrared absorption and re-emission term. Positive forcing occurs when the two are reversed and infrared warming and re-emission exceed scattering back to space. In contrast, all clouds cause a positive nighttime TOA value, with an infrared term alone and no compensating solar albedo term. This dual property makes cirrus distinct, and why it's crucial to understand how well radiative transfer models are resolving their TOA CRE properties.

49 The burgeoning satellite and ground-based era of atmospheric monitoring
50 (Sassen and Campbell 2001; Campbell et al. 2002; Welton et al. 2002; Nazaryan, et
51 al. 2008; Sassen et al. 2008) has led to a wealth of new data for looking at global
52 cirrus cloud properties. In particular, TOA CRE, or at the surface (SFC), are evaluated
53 by means of radiative transfer modeling, designed with different degrees of
54 complexity. What is not yet known is how the relative simplicity of some models
55 translates to a relative retrieval uncertainty, given that the CRE effect of cirrus
56 clouds, at both the ground and TOA, are typically on the order of 1 W m^{-2} (e.g.,
57 Campbell et al. 2016; Lolli et al. 2017). Whereas some studies show the relative
58 uncertainty of such models as static percentages (Corti and Peter, 2009), the
59 absolute magnitude of uncertainty with respect to cirrus CRE is necessary to
60 understand whether or not they fit within acceptable tolerance thresholds sufficient
61 for quantitative use. Further, given the sensitivity in the sign of net annual cirrus
62 cloud daytime TOA CRE specifically (Campbell et al. 2016), it's plausible that some
63 simpler models are routinely aliasing positive versus negative TOA CRE.
64 Corti and Peter (2009; CP) describe a simplified radiative transfer model that
65 relies upon a constrained number of input parameters, including surface
66 temperature, cloud top temperature, surface albedo, layer cloud optical depth, and
67 the solar zenith angle. CP simplifies drastically the framework of the Fu-Liou-Gu
68 radiative transfer model (Fu and Liou 1992; Gu et al. 2003; Gu et al., 2011; FLG), for
69 instance, through a parameterization of the longwave and shortwave fluxes derived
70 from the FLG model calculations for realistic atmospheric conditions. Moreover, CP
71 does not directly consider gaseous absorption. The model has increasingly been

used to assess cirrus cloud radiative effects (Kothe et al. 2011; Kienast-Sjögren et al. 2016; Burgeois et al. 2016) from lidar measurements, owing to its relative simplicity and lower computational burden compared with a model like FLG.

To date, CP model performance vs. FLG model has been evaluated for sensitivities only to simulated synthetic clouds and never on real measurements, especially those collected over long periods (Corti and Peter 2009). Such evaluation, however, can readily be conducted using the unique NASA Micro Pulse Lidar Network (MPLNET; Welton et al. 2002; Campbell et al. 2002; Lolli et al. 2013; Lolli et al., 2014), established in 1999 to continuously monitor cloud and aerosol physical properties (Wang et al., 2012, Pani et al., 2016).

The objective of this technical note is to then assess differences between CP and FLG in terms of net annual daytime TOA CRE. CP and FLG model performance are evaluated using MPLNET datasets collected from Singapore in 2010 and 2011, a permanent tropical MPLNET observational site, and at Greenbelt, Maryland in 2012, a midlatitude site. Our goal is to more appropriately characterize the sensitivities of CP relative to what is generally considered a more complex, and presumably more accurate, model, with the hopes of better understanding relative uncertainties, and thus interpreting whether such uncertainties are appropriate for long-term global cirrus cloud analysis.

2. Method

FLG is a combination of the delta four-stream approximation for solar flux calculations (Liou et al. 1988) and a delta-two–four-stream approximation for IR

flux calculations (Fu et al. 1997), divided into 6 and 12 bands, respectively. It has been extensively used to assess net cirrus cloud daytime radiative effects, most recently for daytime TOA forcing characteristics within MPLNET datasets at both Greenbelt, Maryland and Singapore, respectively (Campbell et al. 2016; Lolli et al. 2017). The results from these studies have led to the hypothesis of a meridional gradient in cirrus cloud daytime TOA radiative forcing existing, with daytime cirrus clouds producing a positive daytime TOA CRE at lower latitudes that reverses to a net negative daytime TOA CRE approaching the non-snow and ice-covered polar regions. They estimate absolute net cirrus daytime TOA forcing term between 0.03 and 0.27 W m^{-2} over land at the mid-latitude site, which ranges annually between 2.20 - 2.59 W m^{-2} at Singapore. The key here to this phenomenon is the possible oscillation of the net daytime TOA CRE term about zero, which is believed to vary by a maximum +/- 2 W m^{-2} in absolute terms (i.e. normalized for relative cirrus cloud occurrence rate and total daytime percentage locally), after accounting for polar clouds that should be net cooling elements and varying surface albedos over land and water exclusively (i.e., not ice). Resolving such processes thus requires relatively high accuracy in radiative transfer simulations.

To calculate daytime cirrus cloud radiative effects from MPLNET datasets, the lidar-retrieved single layer cirrus cloud extinction profile (Campbell et al. 2016; Lewis et al., 2016, Lolli et al., 2016, Lolli et al., 2017) is transformed into crystal size diameter (using the atmospheric temperature profile) and ice water content (*IWC*) profiles using the parameterization proposed by Heymsfield et al. (2014). Those parameters, at each range bin, are input into FLG. The thermodynamic atmospheric

profiles, together with ozone concentrations are obtained with a temporal resolution of +/- 3 hr, from a meteorological reanalysis of the NASA Goddard Earth Observing System Model Version 5.9.12 (GEOS-5). In contrast, for a given cloud case, the corresponding cloud and atmospheric CP input parameters are explicitly the land/ocean surface temperature, the cloud top temperature, the surface albedo, the cloud optical depth for the specific layer and the solar zenith angle.

Calculations here are performed for the same MPLNET observational sites, Singapore and Greenbelt, Maryland (i.e., NASA Goddard Space Flight Center; GSFC). For the former site, two different values of the surface albedo, which is a common input parameter in both models, are fixed at 0.12 and 0.05, respectively, as Singapore is a metropolitan area completely surrounded by sea. This allows us to more reasonably characterize forcing over the broader archipelago of Southeast Asia, and follows the experiments described by Lolli et al. (2017). . At NASA GSFC, only a single over-land albedo is used, though one that varies monthly between 0.12-0.15 based on climatology.

Here, we reconsider these results by first intercomparing those solved with FLG and CP for net daytime TOA CRE over a practical range of cloud optical depth (COD). As described in both Campbell et al. (2016) and Lolli et al. (2017), daytime is specifically defined in these experiments as those hours where incoming net solar energy exceeds that outgoing. Only under such circumstances can the net TOA CRE term become negative. Otherwise, it is effectively nighttime, as the term is positive and all clouds induce a warming TOA term. Nighttime results will instead be

considered as context to understanding net diurnal differences between the models when examining the GSFC dataset.

3. Intercomparisons

The daytime cirrus net TOA CRE, normalized by corresponding occurrence frequency, in this case as a function of COD, was evaluated at Singapore (1.3 N, 103.8 E, 20 m above mean sea level) and GSFC (38.9 N, 76.8 W, 39 m above mean sea level) for both FLG and CP. The method to estimate MPLNET cirrus cloud optical properties is described in Lewis et al. (2015) and Campbell et al. (2016), for both 20 and 30 sr solutions from the unconstrained single-wavelength elastic lidar equation at 532 nm (Campbell et al. 2016). The latter constraint provides "bookend" estimates for TOA CRE designed to approximate system variance. For both models, the daytime cirrus cloud net TOA CRE is calculated as the difference of two model computations using different assumed states (cloudy sky minus cloud and aerosol particulate-free conditions) to isolate the distinct cirrus cloud impact alone (in $W\ m^{-2}$).

3.1 Model sensitivities

An initial sensitivity study was carried out to evaluate how the input parameters, and eventually their uncertainties, influence the net TOA CRE calculations. Results are summarized in Table 1. Model input parameter sensitivities were investigated for surface albedo, COD, land/ocean surface temperature and cloud top temperature. Table 1 shows how much net, SW and LW fluxes change by varying each individual parameter alone. For instance, changing

163 the surface albedo from 0.12 to 0.14 and keeping the other three parameters fixed
164 produces similar changes in both models (26% for CP model and 25% for FLG
165 model). Changing COD from 1 to 1.1 produces a change of 16% for CP and 21% for
166 FLG. Changing surface temperature and cloud top temperature of 1K produces
167 respective changes of 10% and 7% for CP and 7% and 6% for FLG. Though subtle,
168 the models exhibit some differences in variance relative to the input parameters
169 required to initialize them.
170
171 *3.2 Singapore (2010-2011)*
172 FLG and CP were compared over a total of 33072 total daytime single layer
173 cirrus clouds at Singapore from 2010 to 2011. Figures 1, 2, 3 and 4 reflect
174 histograms of cirrus cloud relative frequency and net annual daytime TOA CRE
175 normalized by corresponding frequency, for both surface albedo values of 0.05 (Fig.
176 3 and 4; i.e., over sea) and 0.12 (Fig. 1 and 2; i.e. over land) at 0.03 COD resolution
177 from 0 to 3. This latter range was chosen as consistent with Sassen and Cho (1992),
178 and the nominal effective COD range corresponding with cirrus cloud occurrence.
179 Note, since a common cloud sample is used, the 20 sr samples vary in COD between
180 only 0 and approximately 1 in contrast to the 30 sr sample topping out at 3. The
181 observed differences in net radiative effect can be ascribed to the different lidar
182 ratio. The results here mirror the work of Berry and Mace (2014) who first
183 recognized the significance of optically-thin cirrus influencing the net normalized
184 term so greatly.

185 Intercomparison of net daytime TOA CRE vs. COD over the ocean at 20 sr
186 shows an overall forcing of 1.34 W m^{-2} for CP and 0.48 W m^{-2} for FLG. At 30 sr, we
187 obtain -0.89 W m^{-2} from CP and -0.37 W m^{-2} for FLG. The overall CP net TOA CRE is
188 greater in absolute magnitude than FLG by a maximum difference of 65%. This
189 value is obtained by taking the ratio between yearly CRE from FLG over CP and then
190 the percentage difference. Over land (urban environment), CP net daytime TOA CRE
191 are higher than the FLG model by 30% (CP = 4.20 W m^{-2}, FLG=2.98 W m^{-2} at 20 sr;
192 CP=4.43 W m^{-2} and FLG=3.35 W m^{-2} at 30 sr). The COD value at which cirrus begin
193 cooling the earth-atmosphere system, moving toward higher COD, is systematically
194 shifted towards higher values for CP with respect to FLG. This is particularly evident
195 over ocean at 20 sr where there is a shift of 0.25 in COD (0.6 for CP and 0.35 for FLG;
196 Fig. 3).
197 To better understand the different outputs between the two models, a scatter
198 plot between from FLG barplot entries is shown in Figs. 2 and 4 (30 sr solution), and
199 the corresponding CP barplot values are plotted, over land and over ocean, in Figs. 5
200 and 6. The blue line represents the actual linear data regression, while the red line
201 represents an ideal case (i.e., slope=1, intercept=0). If the two radiative transfer
202 models show identical results regarding CRE, all the points should lie on the blue
203 line. The red line instead represents the actual regression line, or a relative measure
204 of how much the two models differ.
205 From Figs. 5 and 6, the FLG-derived net daytime CP TOA CRE values are
206 systematically greater in absolute value than the corresponding FLG values by 60%.
207 More in detail CP TOA CRE of 1 Wm^{-2} corresponds with FLG values ranging from

208 0.57 Wm^{-2} to 0.59 Wm^{-2}. On the contrary, the bias (or the intercept from the linear
209 regression) shows higher variability depending on the surface type underlying the
210 cirrus cloud (land versus ocean). This indicates that when a cirrus cloud shows a
211 neutral effect (0 Wm^{-2}) for CP model, FLG model solutions range from -0.05 (land)
212 to -1.1 Wm^{-2} (ocean),. This implies that characterization of cirrus cloud warming or
213 cooling effects depend on the model.

214 *3.4 Greenbelt, Maryland 2012*

215 To limit potential assessment ambiguity based on a single-site analysis, we
216 performed a second model comparison using the 2012 NASA GSFC dataset. A
217 summary of this dataset and net daytime TOA CRE results can be found in Campbell
218 et al. (2016). As this site in land-locked, only the single albedo was, again, used,
219 though varied monthly based on climatological passive satellite estimates. 21107
220 daytime cirrus cloud profiles were considered. Shown in Figure 6 (upper panel) are
221 the total net TOA CRE vs. COD at 30 sr, for CP (-2.59 Wm^{-2}) against FLG (0.05 Wm^{-2}).
222 A relative differencing here is impractical. Suffice however, this is a significant
223 difference, and the sign of the net daytime forcing term is in direct question between
224 the two.

225 With this NASA GSFC dataset, we further consider an additional 32185
226 nighttime cirrus cloud cases within the analysis (Fig. 6, lower panel). The thought
227 here is that, relative to prior estimates of CP uncertainty compared with more
228 complex models, a diurnal average would be likely to produce a different, and
229 plausibly closer, relative agreement consistent with prior studies. That is, since
230 during for most of the period we define here as night there is no solar input, a

231 simplification of the infrared forcing terms and parameterizations alone would
232 potentially yield a closer comparison between the two models. For the NASA GSFC
233 dataset, we solved a relative net nighttime TOA CRE of 29.1 Wm^{-2} with FLG
234 compared with 21.0 Wm^{-2} with CP, or a relative difference approaching 50%..
235 Summarized in Table 2 are the discrepancies in terms of CRE at both observational
236 sites.

237 It is useful at this point to discuss some of the potential elements driving
238 these differences. The larger discrepancies between the two models are likeliest
239 ascribed to the parameterization of three specific parameters in the CP model: the
240 first two, σ^* and k^* (Eq. 2 of Corti and Peter, 2009) are two approximated
241 parameters for the Stefan-Boltzmann constant and the surface temperature
242 exponent estimated from radiative calculations and used to calculate the outgoing
243 longwave earth radiation. The last parameter, γ^* (again obtained from a regression
244 analysis), is related to the asymmetry factor of cloud droplets and used to calculate
245 the cloud reflectance of shortwave radiation (Eq. 11 in Corti and Peter; 2009). We
246 speculate that, though the analysis is left to a future study on broader uncertainties
247 in modeling ice radiative properties inherently with any model, these parameters
248 are not the constants ascribed by CP, but that their values instead change with
249 respect to season and latitude.

250 The 20% relative model accuracy claimed in Corti and Peter (2009) may be
251 verified for special conditions in tropical latitudes, where the three parameters
252 discussed above are well optimized. But, that is clearly not found from our study.
253 Corti and Peters (2009) expressly stated that they used fixed values for those three

parameters (i.e., σ^* and k^* in Eq. 2 and γ^* in Eq. 11 in Corti e Peter, 2009) again using regression analysis, but this shouldn't be the case, as net TOA CRF is very sensitive to those parameters. For example, varying water vapor concentrations in the atmosphere can be the responsible of a difference up to 25 Wm^{-2} (for temperatures at the surface higher than 288K) in clear-sky earth longwave radiation at Singapore, as stated in Corti and Peter (2009; Fig. 1). In our analysis we verified that, over one year, the land surface temperature is higher than 288K 66% of the time. For this reason, to assess if land surface temperature is responsible for these larger discrepancies, we reproduced Fig. 6 (upper panel) masking out all cases corresponding with land surface temperatures higher than 288 K at Greenbelt (in Singapore those temperatures are mostly during nighttime). Shown in Figure 7 are the results of the analysis. CP and FLG radiative transfer models in this range of temperature are in much better agreement (NET CP = -8.06 Wm^{-2}; NET FLG -8.65 Wm^{-2}), within 6%.

We advise that those looking to apply CP to long-term climate/cirrus cloud study should carefully analyze the relevance of these settings to their given experiment before directly applying the model, especially when land surface temperatures are warmer than 288K.

4. Conclusions

Annual single-layer cirrus cloud top-of-the-atmosphere (TOA) radiative effects (CRE) calculated from the Corti and Peter (2009) radiative transfer model

277 (CP) are compared with similar results from the more complex, and presumably
278 more accurate, Fu-Liou-Gu (FLG) radiative transfer model. The CP model calculates
279 CRE using a parameterization of longwave and shortwave fluxes that are derived
280 from real measurements optimized for a tropical environment through a regression
281 analysis to simplify the radiative calculations. Values for these parameterizations,
282 as suggested in Corti and Peter (2009), lead to relative differences in TOA CRE that
283 far exceed the stated 20% in the original manuscript. This includes parsing results
284 out for daytime, nighttime or diurnal averages. It is believed that specific
285 parameterizations with the simplified model cannot be considered global constants,
286 as originally defined for CP, but that they should be carefully evaluated on single
287 case basis for each experiment. Moreover we find that the land surface temperature
288 is responsible for significant discrepancies when larger than 288K, because the
289 original CP regression analysis is less accurate for larger temperatures. However, CP
290 uses less input parameters compared with FLG, making it practically and
291 computationally more efficient, particularly for large climate datasets. This is the
292 first time, however, that the two models are compared using long-term cirrus clouds
293 datasets, as opposed to synthetic datasets, with experiments conducted using NASA
294 Micro Pulse Lidar datasets collected at Singapore in 2010 and 2011 (Lolli et al.
295 2017) and Greenbelt, Maryland in 2012.

296 Net daytime TOA CRE was evaluated versus cloud optical depth (COD) for
297 steps of 0.03 (COD range: 0-1) at 20 sr and for steps of 0.1 at 30 sr (COD range: 0-3)
298 for both the Singapore and Greenbelt, Maryland datasets. Our findings suggest that
299 the difference in annual net TOA CRE between the two models approaches 65% in

one experiment at Singapore. At Greenbelt, Maryland, the sign of the net annual daytime TOA CRE term differs, and the absolute difference varies between by nearly 2.5 Wm^{-2}. Differences in the sign of the net TOA forcing term, however, are most worrying. Since cirrus clouds are the only cloud that can exhibit daytime positive or negative net TOA CRE, subtle differences in absolute magnitude are less important than whether or not the clouds are inducing a cooling or forcing term in the TOA radiation budget.

In spite of this comparison, even if we reasonably speculate that FLG is the more accurate model overall, because of its relative complexity compared with CP, we are still missing regular comparisons of FLG with real observational data. Thus, the practical gains to long-term application of a simplified model like CP cannot be overstated, given lower computational demands. However, we believe that the results from this study are noteworthy because they show that the differences between the two models are significant. With respect to cirrus annual net daytime TOA CRE, and given the perspective on their global distribution described by Campbell et al. (2016) and Lolli et al. (2017), these sensitivities can lead to completely different conclusions about global cirrus TOA forcing effects. Therefore, in future work, it is imperative on the community to continue understanding and refining the global parameterizations used in all radiative transfer models regarding cirrus. Continued intercomparisons between models with real observation both at ground (using flux measurements), in situ (aircraft measurements) and at TOA (using satellite-based measurements,) remain critical interests.

Acknowledgements

This study and the NASA Micro Pulse Lidar Network (MPLNET) are supported by the NASA Radiation Sciences Program (H. Maring). Author JRC acknowledges the Naval Research Laboratory Base Program (BE033-03-45-T008-17) and support of NASA Interagency Agreement NNG15JA17P on behalf of MPLNET.

References

Berry, E., and G. G. Mace, 2014: Cloud properties and radiative effects of the Asian summer monsoon derived from A-Train data. J. Geophys. Res. Atmos., 119, doi:10.1002/2014JD021458.

Bourgeois, Q. *et al.* 2016: Ubiquity and impact of thin mid-level clouds in the tropics. *Nat. Commun.* 7:12432 doi: 10.1038/ncomms12432

Campbell, S. Lolli J. Lewis, Y. Gu, E. Welton, 2016 "Daytime Cirrus Cloud Top-of-Atmosphere Radiative Forcing Properties at a Midlatitude Site and their Global Consequence" *J. Applied Meteor. Climat*, http://dx.doi.org/10.1175/JAMC-D-15-0217.1

Campbell, et al., 2002," "Aerosol Lidar Observation at Atmospheric Radiation Measurement Program Sites: Instrument and Data Processing", J*. Atmos. Oceanic Technol.*, 19, 431-442

Comstock, J.M., T.P. Ackerson (2001), G. G. Mace:,"Cirrus radiative properties in the tropical western pacific. *Eleventh ARM Science Team Meeting Proceedings*, Atlanta, Georgia, March 19-23.

Corti, T. and Peter, T., 2009: "A simple model for cloud radiative forcing", *Atmos. Chem. Phys.*, 9, 5751-5758, doi:10.5194/acp-9-5751-2009

Dionisi, D., Keckhut, P., Liberti, G. L., Cardillo, F., and Congeduti, F., 2013: Midlatitude cirrus classification at Rome Tor Vergata through a multichannel Raman–Mie–Rayleigh lidar, Atmos. Chem. Phys., 13, 11853-11868, doi:10.5194/acp-13-11853-2013.

352 Fu, Q., K. N. Liou, 1992, "On the correlated *k*-distribution method for radiative
353 transfer in nonhomogeneous atmospheres", *J. Atmos. Sci.*, 49, 2139–2156,
354 1992.
355 Gu, Y., J. Farrara, K. N. Liou, and C. R. Mechoso, 2003: Parameterization of cloud-
356 radiation processes in the UCLA general circulation model. *J. Climate*, 16,
357 3357-3370.
358 Gu, Y., K. N. Liou, S. C. Ou, and R. Fovell, 2011: Cirrus cloud simulations using WRF
359 with improved radiation parameterization and increased vertical resolution.
360 *J. Geophys. Res*. 116, D06119, doi:10.1029/2010JD014574
361 Heymsfield, A., D. Winker, M. Avery, M. Vaughan, G. Diskin, M. Deng, V. Mitev, and R.
362 Matthey, 2014: Relationships between ice water content and volume
363 extinction coefficient from in situ observations for temperatures from 0° to
364 −86°C: Implications for spaceborne lidar retrievals. *J. Appl. Meteor. Climatol.*,
365 53, 479–505
366 Immler, F., Treffeisen, R., Engelbart, D., Krüger, K., and Schrems, O. 2008: "Cirrus,
367 contrails, and ice supersaturated regions in high pressure systems at
368 northern mid latitudes", *Atmos. Chem. Phys.*, 8, 1689-1699, doi:10.5194/acp-
369 8-1689-2008.
370 IPCC: Climate Change 2013 – The Physical Science Basis, Working Group I
371 Contribution to the Fifth Assessment Report of the Intergovernmental Panel
372 on Climate Change, edited by: Inter- governmental Panel on Climate Change,
373 Cambridge University Press, Cambridge, UK and New York, NY, USA, 2014.

374 Khvorostyanov V. I. and K. Sassen, 1998: Cirrus Cloud Simulation Using Explicit
375 Microphysics and Radiation. Part I: Model Description. J. Atmos. Sci., 55,
376 1808–1821
377 Kienast-Sjögren, E., Rolf, C., Seifert, P., Krieger, U. K., Luo, B. P., Krämer, M., and Peter,
378 T.: Climatological and radiative properties of midlatitude cirrus clouds
379 derived by automatic evaluation of lidar measurements, Atmos. Chem. Phys.,
380 16, 7605-7621, doi:10.5194/acp-16-7605-2016, 2016.
381 Kothe, S., Dobler, A., Beck, A. and Ahrens, B., 2011. The radiation budget in a regional
382 climate model. *Climate dynamics*, *36*(5-6), pp.1023-1036.
383 Kuo-Nan Liou, 1986: Influence of Cirrus Clouds on Weather and Climate Processes:
384 A Global Perspective. Mon. Wea. Rev., 114, 1167–1199.
385 Lolli, S., Campbell, J. R., Lewis, J. R., Gu, Y., Marquis, J. W., Chew, B. N., ... & Welton, E. J.
386 (2017). Daytime Top-of-the-Atmosphere Cirrus Cloud Radiative Forcing
387 Properties at Singapore. *J. of App. Met. and Clim.56*(5), 1249-1257.
388 Lolli S., J. Lewis, R. Campbell, Y. Gu, E. Welton, 2016, "Cirrus Cloud Radiative
389 Characteristics from Continuous MPLNET Profiling at GSFC in 2012", *Óptica*
390 *pura y aplicada,* Vol. 49 (1), 1-6,doi:10.7149/OPA.49.1.1.
391 Lolli S. et al, 2013a, "Evaluating light rain drop size estimates from multiwavelength
392 micropulse lidar network profiling.,"*J. Atmos. Oceanic Technol.*, **30**, 2798–
393 2807.
394 Lolli S. et al. 2014. "High Spectral Resolution Lidar and MPLNET Micro Pulse Lidar
395 aerosol optical property retrieval intercomparison during the 2012 7-SEAS
396 field campaign at Singapore." *Proc. SPIE 9246, Lidar Technologies,*

Techniques, and Measurements for Atmospheric Remote Sensing X, 92460C (October 20, 2014); doi:10.1117/12.2067812.

Lewis, J. R., J. R. Campbell, P. C. Haftings and E. J. Welton, 2015: Overview and analysis of the MPLNET Version 3 cloud detection algorithm. *J. Atmos. Oceanic Technol.,* submitted

Min, M., P. Wang, J. R. Campbell, X. Zong, and Y. Li, 2010, "Midlatitude cirrus cloud radiative forcing over China", J. Geophys. Res., 115, D20210, doi:10.1029/2010JD014161.

Nazaryan, H., M. P. McCormick, and W. P. Menzel, 2008, "Global characterization of cirrus clouds using CALIPSO data", J. Geophys. Res., 113, D16211, doi:10.1029/2007JD009481.

Pani, S. K., S.-H. Wang, N.-H. Lin, S.-C. Tsay, S. Lolli, M.-T. Chuang, C.-T. Lee, S. Chantara, and J.-Y. Yu, 2016" Assessment of aerosol optical property and radiative effect for the layer decoupling cases over the northern South China Sea during the 7-SEAS/Dongsha Experiment" J. Geophys. Res. Atmos., 120, doi: 10.1002/2015JD024601

Sassen, K. and J. R. Campbell, 2001: A Midlatitude Cirrus Cloud Climatology from the Facility for Atmospheric Remote Sensing. Part I: Macrophysical and Synoptic Properties. J. Atmos. Sci., 58, 481–496,

Sassen, K., Z. Wang, and D. Liu, 2008, "Global distribution of cirrus clouds from CloudSat/Cloud-Aerosol Lidar and Infrared Pathfinder Satellite Observations (CALIPSO) measurements", J. Geophys. Res., 113, D00A12, doi:10.1029/2008JD009972.

420 Soden, B. J., and L. J. Donner (1994), Evaluation of a GCM cirrus parameterization
421 using satellite observations, J. Geophys. Res., 99(D7), 14401–14413,
422 doi:10.1029/94JD00963.
423 Wang, S. H., S. Tsay, N. Lin, S. Chang, C. LI, E. J. Welton, B. N. Holben N. C. Hsu, W. K.
424 Lau, S. Lolli C. Kuo, H. Chia, C. Chiu, C. Lin, S. W. Bell, Q. Ji, R. A. Hansell, G.
425 Sheu, K. Chi, and C. Peng. 2012. "Origin, transport, and vertical distribution
426 of atmospheric pollutants over the northern South China Sea during the
427 7SEAS/Dongsha experiment." Atmos. Environment, Vol. 78, 124-133
428 Welton, E. J., et al., 2002: Measurements of aerosol vertical profiles and optical
429 properties during INDOEX 1999 using micropulse lidars. *J. Geophys. Res.*,
430 107, 8019,
431

FIGURES

FIGURE 1 Analysis over land (Albedo=0.12) for 20sr solution. CRE vs. COD is weighted by occurrence frequency for Corti and Peter(red) and FLG (blue) models over 2010-2011

FIGURE 2 Analysis over land (Albedo=0.12) for 30sr solution. CRE vs. COD is weighted by occurrence frequency for Corti and Peter(red) and FLG (blue) models on 2010-2011.

FIGURE 3 Same as Figure 1, but over the ocean (Albedo=0.05)

FIGURE 4 Same as Figure 2, but over the ocean (Albedo=0.05)

FIGURE 5 Scatter plot and linear regression for 30sr solution for FLG and CP CRE in 2010-2011 over land (upper panel) and ocean (lower panel)

FIGURE 6 Analysis on 2010 dataset from MPLNET GSFC observational site for 30sr solution daytime (upper panel) and nighttime (lower panel).

FIGURE 7 Same as Figure 6, taking out those measurements with a land surface temperature $T_{surf} > 288K$

458 Tables

459

NET CP	NET FLG	LW TOA FLG	SW TOA FLG	LW TOA CP	SW TOA CP	
-12.6	-9.4	67.8	-77.2	69	-81.6	Ref
9.3 (26%)	-7 (25%)	67.8	-74.8	69	-78.3	Albedo
-14.7 (16%)	-11.4 (21%)	71.8	-83.2	73.5	-88.2	Cod
-11.3(10%)	-8.7(7%)	68.5	-77.2	70.3	-81.6	Surf Temp
-13.5(6%)	-10(5%)	67.2	-77.2	68.1	-81.6	Cl Top Temp

460 Table 1 Total NET, SW and LW fluxes (W/m^2) at TOA. Sensitivities of CP and FLG
461 radiative transfer models with respect to the surface albedo, cloud optical depth
462 Unperturbed parameters are COD=1, Surface albedo=0.12, T_{surf}=294K Cloud top
463 T_{top}=229K. The variation in net radiative forcing expressed in percentage for each
464 parameter are calculated changing the surface albedo from 0.12 to 0.14, the COD
465 from 1 to 1.1, and augmenting the temperatures of 1K.

466

CRE vs. COD	Land	Ocean
SING 2010-2011	20sr CP=4.20 FLG=2.98 (41%)	20sr CP=1.34 FLG=0.48 (68%)
	30sr CP=4.43 FLG=3.35 (32%)	30sr CP=-0.89 FLG=-0.37 (40%)
GSFC 2012	30sr CP=-2.59FLG=0.07	

467 Table 2 Summary of principal CRE (Wm^{-2}) differences between FLG and CP radiative
468 transfer model depending on year and on land/ocean.

469

Figures

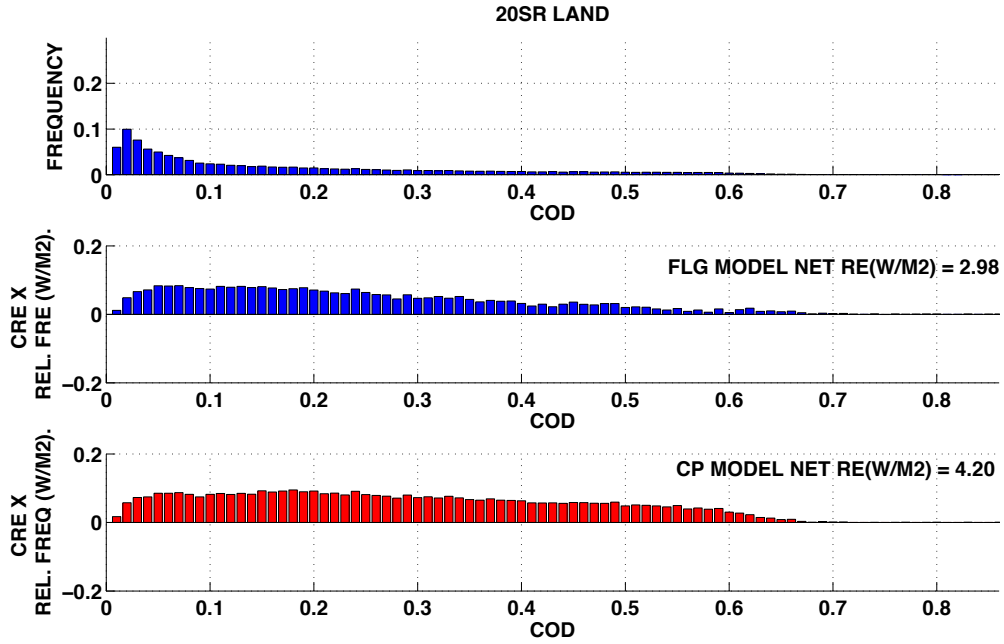

Figure 1 Analysis over land (Albedo=0.12) for 20sr solution. CRE vs. COD is weighted by occurrence frequency for Corti and Peter(red) and FLG (blue) models over 2010-2011

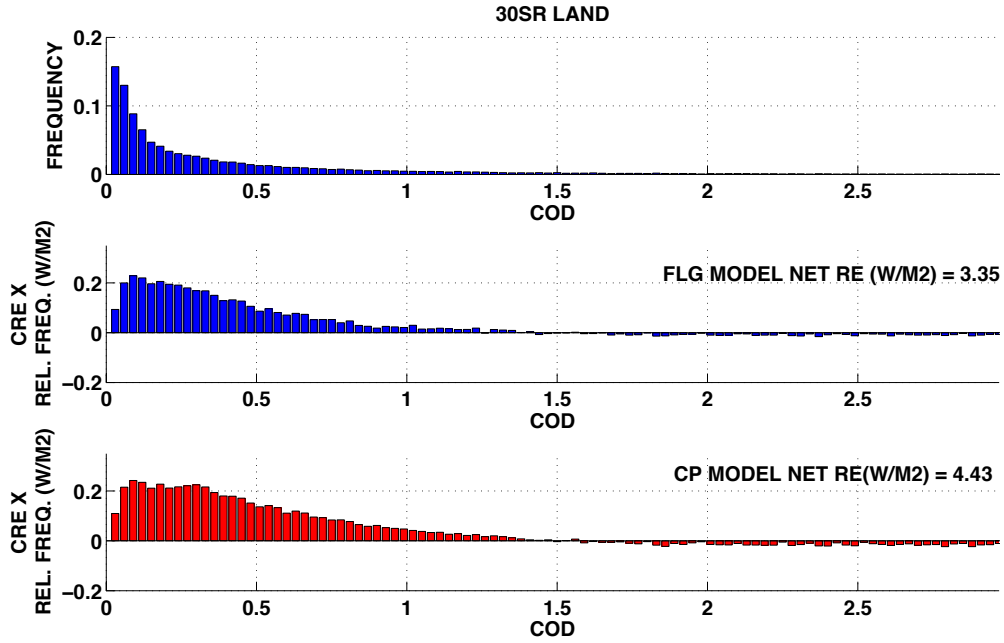

476 **Figure 2** Analysis over land (Albedo=0.12) for 30sr solution. CRE vs. COD is weighted by occurrence
477 frequency for Corti and Peter(red) and FLG (blue) models on 2010-2011.
478

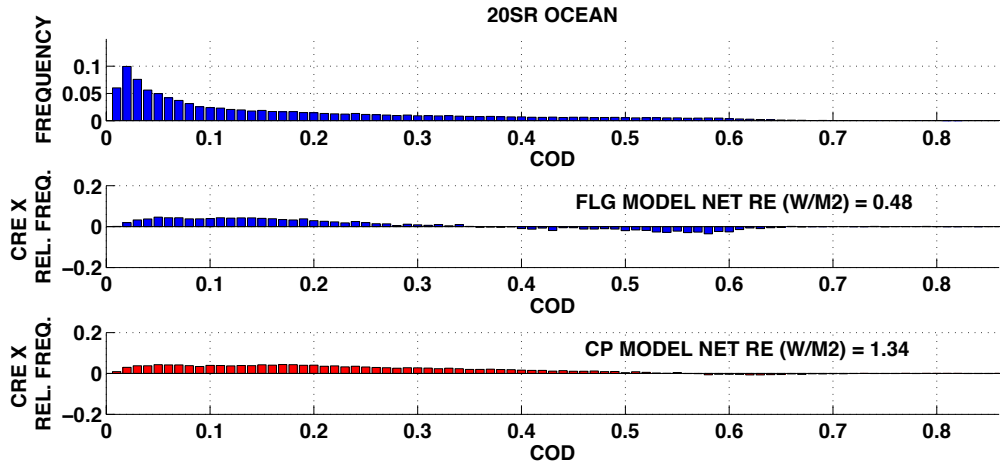

479

480 **Figure 3** Same as Figure 1, but over the ocean (Albedo=0.05)
481

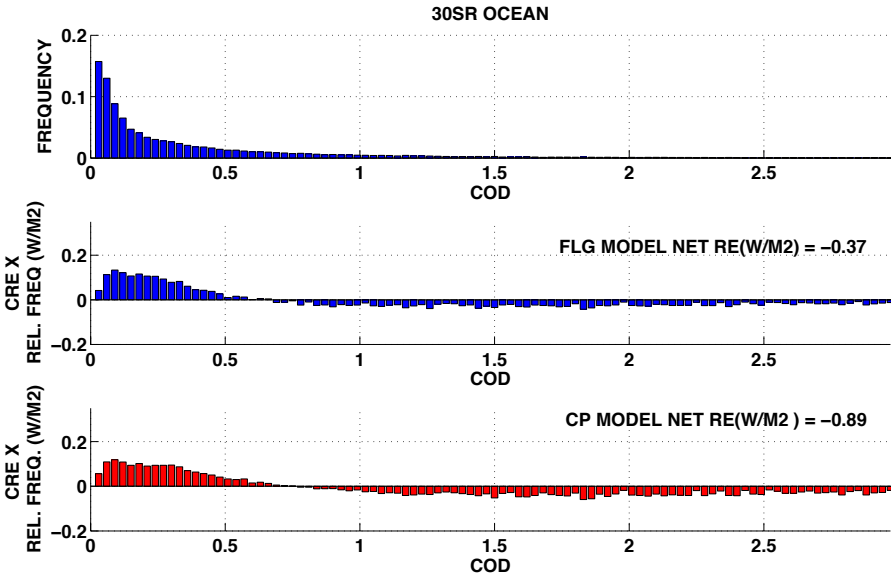

482

483 **Figure 4** Same as Figure 2, but over the ocean (Albedo=0.05)
484

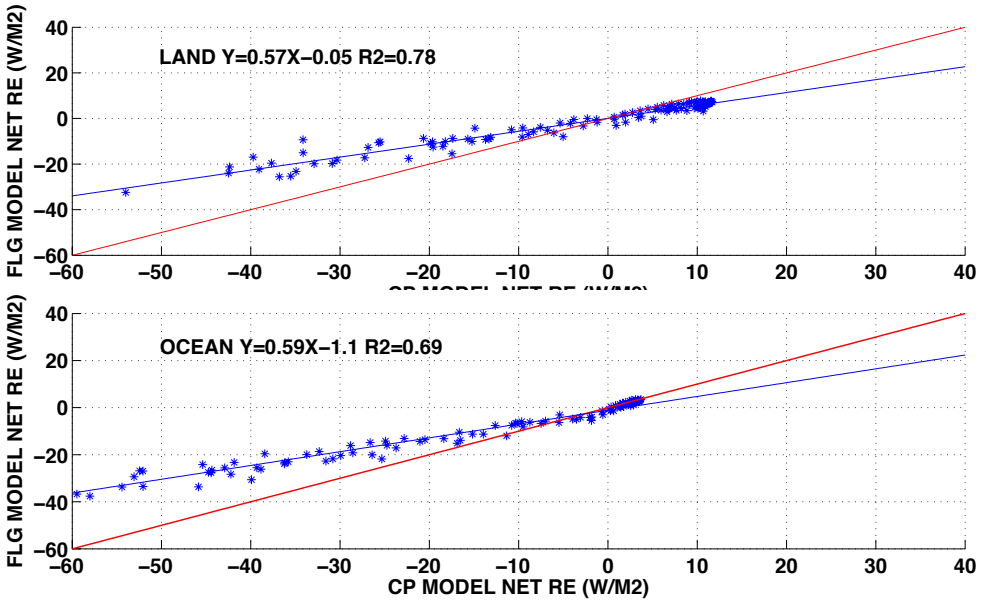

Figure 5 Scatter plot and linear regression for 30sr solution for FLG and CP CRE in 2010-2011 over land (upper panel) and ocean (lower panel)

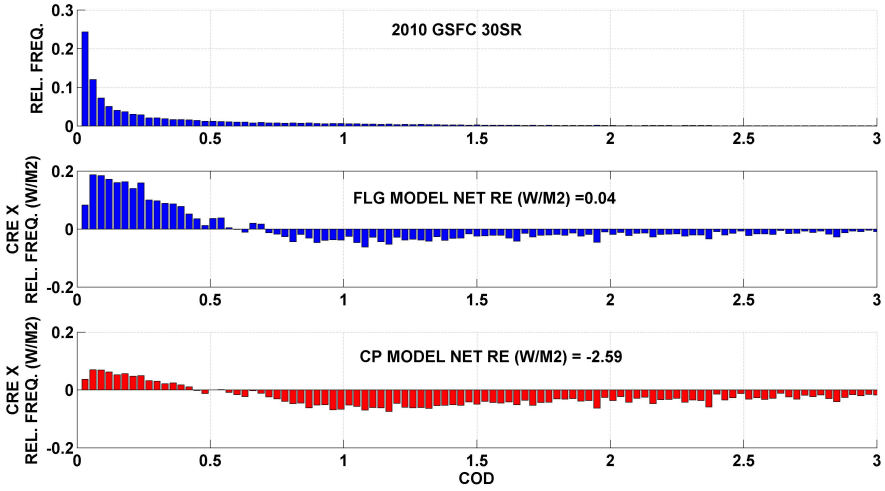

492

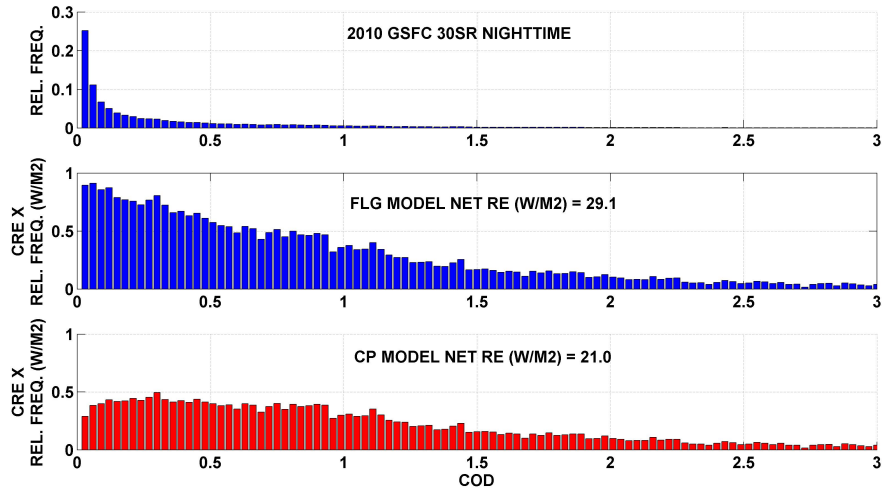

493
494
495 **Figure 6** Analysis on 2010 dataset from MPLNET GSFC observational site for 30sr solution daytime
496 (upper panel) and nighttime (lower panel).
497

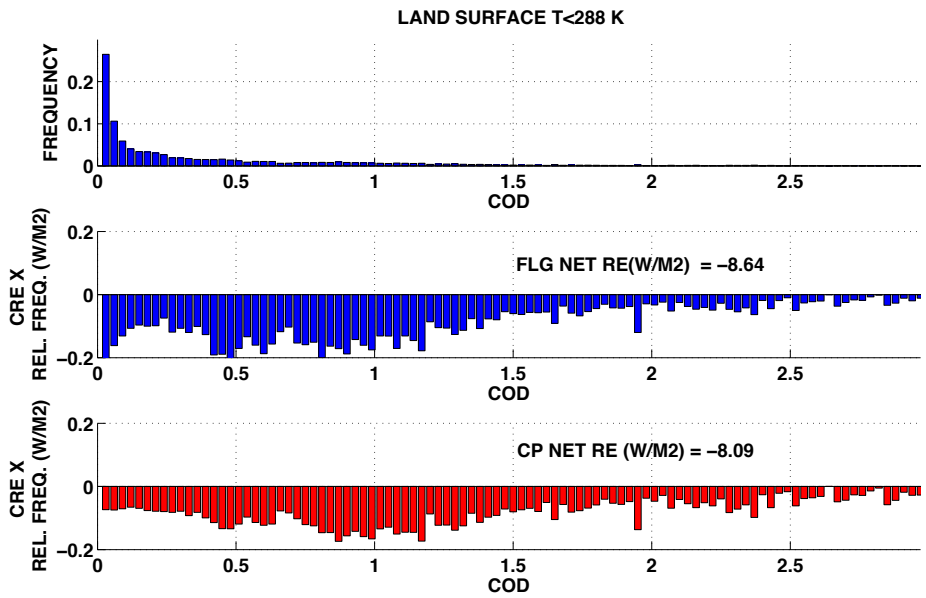

Figure 7 Same as Figure 6, taking out those measurements with a land surface temperature T_{surf} > 288K